Journal of Materials Chemistry B

ROYAL SOCIETY OF CHEMISTRY

PAPER

View Article Online
View Journal | View Issue

Cite this: J. Mater. Chem. B, 2022, 10, 6816

Molecular imprinting as a simple way for the long-term maintenance of the stemness and proliferation potential of adipose-derived stem cells: an *in vitro* study†

Abolfazl Nazbar,[a] Saeed Samani,[b] Sepideh Yazdian Kashani,*[c] Amir Amanzadeh,[a] Shahram Shoeibi[d] and Shahin Bonakdar*[a]

Cells are smart creatures that respond to every signal after isolation and *in vitro* culture. Adipose-derived stem cells (ADSCs) gradually lose their characteristic spindle shape, multi-lineage differentiation potential, and self-renewal ability, and enter replicative senescence after *in vitro* expansion. This loss of cellular function is a serious impediment to clinical applications that require huge numbers of cells. It has been proven that substrates with cell imprints can be applied for stem cells' differentiation into desired cells or to re-culture any cell type while maintaining its ordinary activity. This study demonstrated the application of cell-imprinted substrates as a novel method in the long-term expansion of ADSCs while maintaining their stemness. Here we used molecular imprinting of stem cells as a physical signal to maintain stem cells' stemness. First, ADSCs were isolated and cultured on the tissue culture plate. Then, cells were fixed, and stem cell-imprinted substrates were fabricated using PDMS. Afterward, ADSCs were cultured on these substrates and subjected to osteogenic and adipogenic differentiation signals. The results were compared with ADSCs cultured on a polystyrene tissue culture plate and non-patterned PDMS. Morphology analysis with optical and fluorescence microscopy and SEM images illustrated that ADSCs seeded on imprinted substrates kept ADSC morphology. Alizarin Red S and Oil Red O staining, flow cytometry, and qPCR results showed that ADSC-imprinted substrates could reduce the differentiation of stem cells *in vitro* even if the differentiating stimulations were applied. Also, cell cycle analysis revealed that ADSCs could maintain their proliferation potential. So this method can maintain stem cells' stemness for a long time and reduce the unwanted stem cell differentiation that occurs in conventional cell culture on tissue culture plates.

Received 7th February 2022,
Accepted 16th June 2022

DOI: 10.1039/d2tb00279e

rsc.li/materials-b

1. Introduction

In recent years the application of adult and embryonic stem cells has received special attention in cell therapy and tissue engineering; in many cases, it is impossible to obtain a suitable cell substitute for adult tissues from the patient's adult cells to repair damaged tissues.[1–3] When a stem cell divides in the human body, it may not change its nature or differentiate into a specific cell, such as muscle, red blood, or brain cells. So, stem cells in many tissues serve as a regeneration system to renew damaged cells. Chemical, mechanical, electrical, and surface factors can affect stem cell fate. Despite the conditions causing differentiation into desirable cells, the conditions under which proliferation occurs without differentiation are also necessary. Many researchers have been interested in mesenchymal stem cells (MSCs) to overcome the constraints of employing adult cells in regenerative medicine by considering self-renewal capacity, multi-lineage differentiation potential, and immunosuppressive ability. So, because of their unique characteristics, such as availability, differentiation potential, immune cell evasion, and easy *in vitro* proliferation, MSCs are a promising cell type for regenerative medicine and stem cell therapy.[4] Also, the advantages of using allogeneic instead of autologous cells are essential factors to be considered in cell transplantation methods that can be achieved using MSCs.[5–7]

Intravenous injection of MSCs requires minimal effective dosages of about 70–190 million cells per patient per dose, and

[a] National Cell Bank Department, Pasteur Institute of Iran, Tehran, Iran. E-mail: sh_bonakdar@pasteur.ac.ir
[b] Department of Tissue Engineering and Applied Cell Sciences, School of Advanced Technologies in Medicine, Tehran University of Medical Sciences, Tehran, Iran
[c] Department of Chemical Engineering, Amirkabir University of Technology (Tehran Polytechnic), Tehran, Iran. E-mail: ykashani@aut.ac.ir
[d] Food and Drug Laboratory Research Center (FDLRC), Iran Food and Drug Administration (IFDA), MOH & ME, Tehran, Iran

† Electronic supplementary information (ESI) available. See DOI: https://doi.org/10.1039/d2tb00279e

around 100 million cells are necessary to treat a person weighing 70 kg. However, on the one hand, clinical trials are hampered by the deficient availability of MSCs in isolated samples. For example, MSCs make up just 0.001–0.01% of nucleated cells aspirated from bone marrow.[8,9] Therefore, extensive *in vitro* passaging is needed to expand freshly homogenous MSC populations before clinical applications.[5] On the other hand, isolated adult stem cells may inadvertently differentiate into undesirable cell lineages during *in vitro* continuously culturing in conventional tissue culture plates (TCP),[5] leading to the loss of their normal phenotype.[10] Indeed, biochemical and biophysical cues in the surrounding environment influence cell proliferation and differentiation,[11] and regulate the MSCs' differentiation ability into a specific lineage.[4]

The *in vivo* microenvironment provides numerous regulating stimuli not available in conventional cell culture methods.[12] In native tissues, cells do not live alone and continually sense and interact with the extracellular matrix (ECM).[13] The ECM supports most cellular functions chemically, mechanically, and physically,[13,14] and can determine the fate of stem cells.[15] For large-scale clinical stem cell applications requiring large numbers of stem cells, loss or alteration of cell function is a significant barrier.[9] Although many studies have been performed to mimic the ECM, preparation of an acceptable artificial ECM is not facile.[16]

Because complex topographical niches, such as ECM shape, govern cell activities *in vivo*, the topographic surfaces at the micro and nanoscale can regulate stem cell fate.[17] Previous studies have shown that stem cells can sense changes in nanoscale topographical features, highlighting the role of nanostructured biomaterials' surface free energy in regulating cell fate.[18] For example, for osteogenic differentiation of stem cells, Shi *et al.* made micropatterned PDA-coated parafilms with varied groove widths providing topographic cues for cell control on PDA-coated parafilms.[19] These results support the hypothesis that besides the mechanosensing characteristics such as rigidity or elasticity, cells recognize the topography of their substrates, and surface topography affects stem cell differentiation and fate.[20–26]

Adipose tissue can be obtained from by-products of certain processes, such as esthetic surgery, which was previously considered as biological waste. Thus, using adipose-derived mesenchymal stem cells (ADSCs) avoids many ethical problems associated with bone marrow-derived stem cells.[27] *In vitro* expansion of ADSCs changes their characteristic spindle shape, self-renewal ability, and multi-lineage differentiation potential causing their replicative senescence.[9] For clinical applications, strategies that allow the generation of large numbers of ADSCs parallel to the long-term maintenance of their stemness are required.[28]

The importance of culture substrate properties, such as substrate nanostructures, topography, and stiffness on cell fate, has been evaluated in various studies.[29–34] The most often used substrates for *in vitro* cell culture are tissue culture plates that increase the likelihood of osteogenic differentiation because of the substrate rigidity.[35] So, in stem cell-based regenerative medicine, suitable cell culture platforms providing well-defined biophysical and biochemical properties are needed to mimic the *in vivo* microenvironments,[12] and simulate identical cell proliferation and differentiation conditions.[36] Nonetheless, designing a substrate that will give the required biological cues to drive cells still is challenging.[37]

One of the fundamental areas in regenerative medicine is the responsiveness of stem cells to topographical cues, including micro- and nanoscaled patterns influencing cell fate. Although patterns are frequently employed to enhance cell functions, their mechanisms are not known completely. Furthermore, the concerns of chemical cues, such as growth factors' expensiveness, their short half-life *in vivo*, and the possibility of harmful effects from overdosing, have been solved in topographical patterns.[37]

Molecular recognition is essential in most biological processes because it allows selective and intelligent distinguishing of individual molecules in complex surroundings.[38] Molecular imprinting is a synthetic method that creates biomimetic materials for protein recognition.[39] Molecularly imprinted polymers (MIPs) have been proven to promote cell adhesion and proliferation, are stable in various chemical and physiological conditions and can be used multiple times.[40] MIPs are a popular alternative to natural molecular recognition elements,[38,41] and can mimic the antigen-binding properties of antibodies.[39] Surface imprinting is one of the leading fabrication strategies of MIPs, including different approaches such as soft lithography. In soft lithography, an elastomeric stamp is made by casting a pre-polymer solution, typically polydimethylsiloxane (PDMS) with a relatively low elastic modulus, onto the template. After polymerization and stamp production, specific geometries can be made from nanoscale (30 nm) to micro-scale (100 μm).[36,37]

PDMS has been employed in the imprinting procedure because of its simplicity of fabrication, gas permeability, optical transparency, and low chemical reactivity.[42] Also, against conventional TCP, PDMS has many other advantages such as nontoxicity, adjustable physico-mechanical properties, easy moldability, precision at micro-scale and nanoscale, and low manufacturing costs, which make it desirable as a cell culture substrate.[12] As a substrate to study cell behavior, PDMS provides a better understanding of cell behavior toward stretching,[43] stiffness,[44] mechanical stimulation,[45] and topography.[46–49]

However, the surface hydrophobicity of PDMS has a negative effect on cell adhesion and, consequently, normal cell behaviors and functions.[12] Additionally, because cells and especially stem cells do not intrinsically attach to any surface, some surface modifications are mandatory for PDMS to improve cell attachment and spreading.[50] So, many approaches have tried to alter the PDMS surface somehow to overcome its limitations,[51,52] which can be done by plasma treatment, ECM protein coating, or other molecular coatings. Despite better cell adhesion and spreading acquired *via* these modifications, they are not practical for all cell lines, can be influenced by variable conditions, and cannot ensure the expected demand for the qualified cell source for human therapeutic use.[12]

Some studies have focused on using cellular patterns as biophysical stimulating factors to direct cellular functions in a specific direction. For the first time, Mahmoudi *et al.* prepared a cell-imprinted substrate by PDMS casting and polymerization on mature chondrocytes to induce chondrogenic differentiation in rabbit adipose tissue-derived mesenchymal stem cells.[49] Furthermore, chondrocyte spherical shape-imprinted substrates were used to induce differentiation, redifferentiation, and transdifferentiation. It was discovered that a chondrocyte template might successfully shift MSC and semifibroblast spindle morphology toward spherical morphology. By manipulating the cellular shape, any cells with chondrogenic differentiation potential could be differentiated into chondrocytes.[47] In other studies, osteogenic,[53] keratinogenic,[48] neurogenic,[54–56] and tenogenic[57] differentiation of stem cells was achieved by the imprinting method. Also, the imprinting approach for induced pluripotent stem cells can improve cardiomyogenic differentiation efficiency.[29] Cell imprinting can also reduce or eliminate the requirement for lengthy patient sample analysis.[58] Overall, molecular and cellular imprinting may be a promising way to manipulate cell phenotypes and functions without any chemical cues.

Rather than stem cell differentiation studied in previous reports, this study reveals a novel role of cell-imprinted substrates for maintaining stemness and proliferation potential of ADSCs during their *in vitro* long-term culture for future clinical and tissue engineering applications. Based on published findings of the positive effects of nanotopographies on cell fate, we concluded and expected that the patterns of stem cells could influence cellular behaviors better. Thus we developed ADSC-patterned and non-patterned PDMS substrates and cultured ADSCs on them. Then, we evaluated the effect of the ADSC pattern on maintaining stemness and decreasing osteogenic and adipogenic differentiation for a long time. We hope that our observations encourage other researchers to perform new studies to understand stemness maintenance better.

2. Experimental

2.1. ADSC isolation

The experiments were carried out at the Pasteur Institute of Iran and were approved by the institute's ethics committee (code: IR.PII.REC.1399.005). After signing the consent forms by all patients, adipose tissue was obtained from healthy individuals having a cesarean delivery and preserved at room temperature in DMEM (GIBCO, Scotland) containing 10% (v/v) fetal bovine serum (FBS, GIBCO, Scotland), 100 U mL^{-1} penicillin (Sigma-Aldrich, USA), and 100 μg mL^{-1} streptomycin (Sigma-Aldrich, USA) (complete culture medium).

Based on Iran National Cell Bank's protocols and previously published studies, harvested adipose tissue was rinsed three times with DMEM containing an antibiotic/antimycotic solution (1%, Invitrogen, USA). Then connective tissues and blood vessels were separated, the adipose fragments were washed with phosphate-buffered saline (PBS) solution supplemented by antibiotic/antimycotic agents (1%, Invitrogen, USA), and treated with collagenase type I (0.02 mg mL^{-1}, GIBCO, USA) for 45 minutes at 37 °C. After centrifuging the homogenate at 2000 rpm for five minutes, the deposited cell pellet was suspended and cultured in DMEM supplemented with 10% FBS and 1% Pen/Strep under common cell culture conditions (37 °C, 5% CO_2, in a humidified atmosphere).[2,47,59]

2.2. ADSC characterization

The isolated ADSCs were characterized by flow cytometry with positive and negative CD markers. Additionally, the ADSCs were cultured in osteogenic and adipogenic mediums. Alizarin Red S and Oil Red O were used to stain the fixed cells after 21 days to confirm the osteogenic and adipogenic differentiation potential, respectively.[60] The detailed procedures are as below.

2.2.1. Flow cytometry. Cluster of differentiation (CD) markers are widely used for recognizing and determining cell types, including ADSCs. Flow cytometry was used to look for specific surface markers in ADSCs in this study. After collecting ADSCs by trypsinization at the first passage, the ADSCs were washed with PBS and incubated for 30 minutes in a non-specific blocking solution containing 1% (w/v) bovine serum albumin. After centrifugation and removal of the blocking solution, the ADSCs were treated with fluorescently conjugated mouse anti-human antibodies for 45 minutes, and the expression of the surface markers CD34, CD45, CD105 (BD Biosciences, USA), and CD90 (BioLegend, USA) was evaluated using a BD FACS Calibur flow cytometer (BD bioscience, San Jose, CA, USA) and FlowJo software. CD34 and CD45 are hematopoietic stem cell markers that are not expected to be expressed by MSCs, while the rest are MSC-specific surface markers.[5,61]

2.2.2. Alizarin Red S and Oil Red O staining. Freshly isolated ADSCs were seeded on a tissue culture plate and propagated for 24 hours under common cell culture conditions. To evaluate the osteogenic potential, the ADSCs were cultured in an osteogenic differentiation medium containing high-glucose DMEM supplemented with 10% FBS, 10 mM beta-glycerol-phosphate, 0.1 μM dexamethasone, 50 μg mL^{-1} ascorbic acid, 3.72 mg mL^{-1} sodium bicarbonate, and 1% penicillin/streptomycin/fungizone. Also, the ADSCs were cultured in an adipogenic differentiation medium containing high-glucose DMEM supplemented with 10% FBS, 60 μM 3-isobutyl-1-methylxanthine (IBMX), 3.72 mg mL^{-1} sodium bicarbonate, 1 μM dexamethasone, 0.5 mM indomethacin, 10 μL mL^{-1} insulin, and 1% penicillin/streptomycin/fungizone to evaluate their adipogenic potential.[5] Every three days, the differentiating mediums were exchanged with fresh medium. After 21 days, the cells were rinsed with PBS three times, fixed with 4% paraformaldehyde (Merck, USA), and stained with Alizarin Red S or Oil Red O (Sigma-Aldrich, USA), and morphological transformations were then evaluated by optical microscopy (BEL photonics, Italy).[2]

2.3. Developing cell-imprinted substrates

Freshly isolated ADSCs at a density of 3×10^5 cells per well were seeded in the 6-well tissue culture plate and incubated for one

week. After reaching 90% confluence, the cells were fixed with 4% glutaraldehyde solution for 24 hours and washed with PBS three times. The PDMS casting procedure was performed by pouring the prepared elastomer solution onto the fixed ADSCs and kept at 37 °C for 48 hours. PDMS-based substrate platforms were fabricated by blending PDMS (Sylgard 184 Silicon Elastomer Kit, Dow Corning) with different curing agent weight ratios (curing agent/base polymer = 1 : 10, 1 : 20, 1 : 30, 1 : 40, and 1 : 50). Then the mold was peeled off from the tissue culture plate and rinsed thoroughly with 1 M NaOH solution for 30 minutes to eliminate any residual cell debris and existing chemicals from the imprinted substrates.[2,49,54,55,59]

2.4. Surface characterization of PDMS substrates

Scanning Electron Microscopy (SEM, Philips XL30, Netherlands) images of the substrates were evaluated based on previously published protocols.[2,55]

2.5. ADSC culture on the cell-imprinted substrates

ADSCs were proliferated on the cell-imprinted PDMS, non-patterned PDMS, and tissue culture plate (TCP) as the control, which were called $ADSC_I$, $ADSC_P$, and $ADSC_T$, respectively. The cells (at a density of 4×10^4 cells per sample) were seeded onto the fabricated PDMS-based culture platforms placed in the 6-well plates and tissue culture plates as well. Fresh DMEM supplemented with 10% FBS was added, and exchanged every three days, and the cells were passaged every seven days. Finally, appropriate analyses were carried out considering suitably designed intervals.

2.5.1. Adhesion characterization of cultured ADSCs. After seven days, the adhesion of ADSCs on the imprinted PDMS substrate, non-patterned PDMS, and TCP were evaluated by optical and scanning electron microscopy. Briefly, the supernatant culture medium was discarded slowly, the substrates were rinsed with PBS three times, and the cells were fixed with 4% glutaraldehyde. After two hours, the fixing solution was removed, and gradually increasing ethanol concentrations of 60%, 70%, 80%, 90%, 95%, and 100% were added for 15 minutes each for dehydration. Then the samples were dried at room temperature in an exhaust hood for 30 minutes, and gold-coated, and SEM images were taken using a Philips XL30 (Netherlands) scanning electron microscope.

2.5.2. Cell proliferation assay. For quantitatively evaluating the proliferation of ADSCs, the Alamar Blue assay was carried out after 1, 3, 7, and 14 days of cell culturing on the PDMS-based substrates and TCP. The cells were seeded at 15 000 cells per mL onto the fabricated PDMS-based culture platforms placed in the 24-well plates and TCP for the mentioned time points. The culture medium was removed slowly, and the cells were rinsed gently with PBS to avoid cell detachment, and treated for four hours with a 9 : 1 (v/v) dilution of Alamar Blue in FBS-free DMEM. After incubation, three 150 μL replicates of Alamar Blue-containing solutions were pipetted into a blank 96-well plate, and optical densities at 560 nm excitation and 590 nm emission were read by an ELx808 ELISA reader (BioTek, USA).

2.5.3. Lineage adaptation. To investigate the effect of cell-imprinting on the prevention of or delay in differentiation, the ADSCs seeded on PDMS-based substrates and TCP were subjected to differentiating and non-differentiating conditions. The ADSCs at passage 3 were seeded and cultured on cell-imprinted PDMS, non-patterned PDMS, and TCP for 24 hours under common culture conditions. Then supernatant mediums were removed slowly every three days and replaced with complete culture medium, osteogenic medium, and adipogenic medium for up to 21 days. The treated ADSCs were fixed with 4% paraformaldehyde and stained with Alizarin Red S and Oil Red O to evaluate their osteogenic and adipogenic differentiation potential.

2.5.4. Flow cytometry. Flow cytometry was used to determine the specific surface markers of ADSCs and confirm the positive effect of cell imprinting on long-term maintenance of stemness. ADSCs were cultured on the cell-imprinted PDMS, non-patterned PDMS, and tissue culture plate in complete culture medium after eight passages (eight weeks) and adipogenic medium after three weeks. The expression of surface markers CD105 and CD90 were analyzed by flow cytometry.

2.5.5. ADSC propagation. The ADSCs (at passage 4) were subcultured every seven days up to 21 days on the surfaces of TCP and PDMS-based substrates (5×10^4 cells per sample), collected at the end of passages 5, 6, and 7, and counted using a trypan blue exclusion method to determine the proliferative capability of *in vitro* aging ADSCs. Then the cell population doubling time (CPDT) was calculated as follows:

$$\mathrm{CPDT} = (t - t_i) \times \log\left\{2 \times \left[\log\left(\frac{N_t}{N_i}\right)\right]^{-1}\right\} \qquad (1)$$

where N_i and N_t are the cell numbers at initial seeding (day 0) and at a specific time point t, respectively.[5]

2.5.6. Cell cycle analysis. ADSCs cultured on the cell-imprinted PDMS, non-patterned PDMS, and tissue culture plate were passaged every seven days, and cell cycle analyses were carried out after eight weeks (at passage 8). ADSCs were monodispersed by trypsinization and rinsed with PBS. After adding 70% ethanol as a fixative and putting it in the refrigerator for two hours, the samples were centrifuged, the supernatant was discarded, and cells were washed with PBS. After removing PBS, 1 mL of Propidium Iodide (PI) master mix (40 μL of PI + 10 μL of RNase (DNase free) + 950 μL of PBS) was added to the cells, incubated for 30 minutes and analyzed by flow cytometry.

2.5.7. Morphological characterization. Morphological differences between ADSCs cultured on the cell-imprinted PDMS, non-patterned PDMS, and TCP after eight weeks (at passage 8) were observed by optical and fluorescence microscopy. For optical imaging by BEL INV2 (BEL Engineering, Italy), the cells were washed with PBS and fixed with 4% glutaraldehyde for four hours at 4 °C. For fluorescence imaging by a TCM400 fluorescence microscope (LABOMED, The Netherlands), the ADSCs were washed with PBS, fixed with 4% paraformaldehyde at room temperature for 30 minutes, and labeled with DiI (Sigma-Aldrich, USA) for 15 minutes at 37 °C in darkness.

2.5.8. Gene expression profiling. After eight weeks, total RNA was extracted from the ADSCs cultured on the cell-imprinted and non-patterned PDMS as well as TCP using Total RNA Kit (Yekta Tajhiz Azma, Iran) according to the manufacturer's instructions. Genomic DNA was removed during RNA extraction using DNase I (TaKaRa, Japan). The content and integrity of extracted total RNA were determined by detecting the maximum absorbance at 260 and 280 nm using a NanoDrop One spectrophotometer (Thermofisher, USA). After the synthesis of complementary DNA (cDNA) using One-Step RT-PCR Kit (TaKaRa, Japan), the StepOne equipment (Applied Biosystems, USA) was used to perform the quantitative polymerase chain reaction (qPCR). Each qPCR reaction included 20 μL of mixture solution consisting of 4.5 μL of cDNA, 3.5 μL of sterilized deionized water, 1 nM concentration of each primer (Table 1), and 10 μL of SYBR PCR Master Mix (Takara, Japan). These conditions were used in the cycling: 95 °C for 10 minutes as the holding time (one cycle), denaturation at 95 °C for 30 seconds, followed by annealing/extension at 60 °C for one minute (40 cycles). Finally, the fold change of gene expression was analyzed using REST 2009 software (QIAGEN, Germany) at the significance level of 0.05.

2.5.9. Multipotency evaluation after long-term cell culturing. To assess the effects of the cell-imprinted platform on the multi-lineage differentiation ability, the ADSCs were cultured on a tissue culture plate, non-patterned PDMS, and ADSC-imprinted PDMS for eight passages (eight weeks). Then the ADSCs were trypsinized, cultured in a 24-well plate at a density of 5×10^4 cells per well, and treated with osteogenic and adipogenic mediums for 21 days. Confluent cells were fixed with 4% paraformaldehyde, and stained with Alizarin Red S and Oil Red O, and morphological transformation was represented by optical microscopy (BEL INV2, BEL Engineering, Italy).

2.6. Statistical analysis

All results are presented as mean ± standard deviation. For statistical comparisons between multiple groups, one-way ANOVA on Ranks followed by Tukey's *post hoc* test was done at the significance level of 0.05.

Table 1 Primer sequences used in real-time PCR

Primer	Sequence (5′ → 3′)	
GAPDH	Forward	GAGTCCACTGGCGTCTTCA
	Reverse	TCTTGAGGCTGTTGTCATACTTC
Collagen I	Forward	CGATGGCTGCACGAGTCA
	Reverse	GGTTCAGTTTGGGTTGCTTGTC
PPRγ	Forward	ACGAAGACATTCCATTCACAAG
	Reverse	CTCCACAGACACGACATTCAAT
Osteocalcin	Forward	CAGCGAGGTAGTGAAGAGACC
	Reverse	TCTGGAGTTTATTTGGGAGCAG
CD34	Forward	GCCCAGATCAGCTCCTAACCC
	Reverse	GATCCCTGCTCAACCCCT
CD105	Forward	GCATCCTTCGTGGAGCTACC
	Reverse	GAGGAGTGGTCTGGATCGG
CD90	Forward	ATGAAGGTCCTCTACTTATCCGC
	Reverse	GCACTGTGACGTTCTGGGA

3. Results and discussion

3.1. ADSC characterization

Fig. 1A–D show the characterization of stem cells by flow cytometry with positive and negative CD markers. Flow cytometry analysis revealed that the ADSCs at the first passage could express the MSC-specific markers (CD105 and CD90) well, and the expressions of the hematopoietic markers (CD45 and CD34) were at a low level.[5,62] Fig. 1E and F show the Alizarin Red S and Oil Red O staining after 21-days of culturing in osteogenic and adipogenic mediums. These results confirmed the capability of the ADSCs for differentiating into osteoblast- and adipocyte-like cells demonstrated by deposited calcium compound (Fig. 1E) and lipid droplets (Fig. 1F), respectively.[63] After isolation, to reach the appropriate confluence in a short time, the ADSCs were counted and transferred to culture plates in the desired number to maintain the cells in ideal conditions, less affected by growth and proliferation conditions in tissue culture plates. After culturing for one week in a tissue culture plate, the ADSCs were fixed with 4% glutaraldehyde before pouring PDMS on them. This fixation maintains the cell morphology during the cell-imprinting process.

3.2. Characterization of ADSC-imprinted substrates

Fig. 2 shows the SEM images of imprinted PDMS substrates from different surfaces, including air (PDMS with no imprint), TCP, and ADSCs. SEM evaluations of the cell-imprinted PDMS substrates showed that the imprinting process was performed well, and ADSCs' topography was transferred to the PDMS substrate.

To gain the topography of ADSCs precisely, PDMS must flow slowly during the molding and curing processes, which is dependent on the curing agent/PDMS ratio. It has been shown that there is a relationship between substrate stiffness and stem cell potency. A soft substrate retains the proliferative and differentiating potential of mesenchymal stem cells during long-term expansion.[9,64] Overall, mixtures of different curing agent/PDMS ratios (1 : 10, 1 : 20, 1 : 30, 1 : 40, and 1 : 50) were evaluated to adjust the surface stiffness and better molding. A ratio of 1 : 30 was chosen in this study because it could perform the cell-imprinting process well and could be easily peeled from the plate surface after curing. Diluted mixtures (1 : 40 and 1 : 50 ratios) were not appropriate for the cell-imprinting process because they could not be peeled easily after curing and were torn.

Also, washing the surface of the cell-imprinted substrate with 1 M NaOH removes cell debris and proteins after mold casting, eliminates the effect of these residues on cell fate, and restricts the results and observations to the cellular imprinted template. The X-ray photoelectron spectroscopy (XPS) elemental analysis of the surface of cell-imprinted PDMS substrate confirmed the absence of detectable nitrogen atoms after chemical treatment by NaOH, proving the absence of detectable protein on the surface.[54]

According to the Mahmoudi *et al.* study in which high-resolution AFM analysis was performed for cell-imprinted

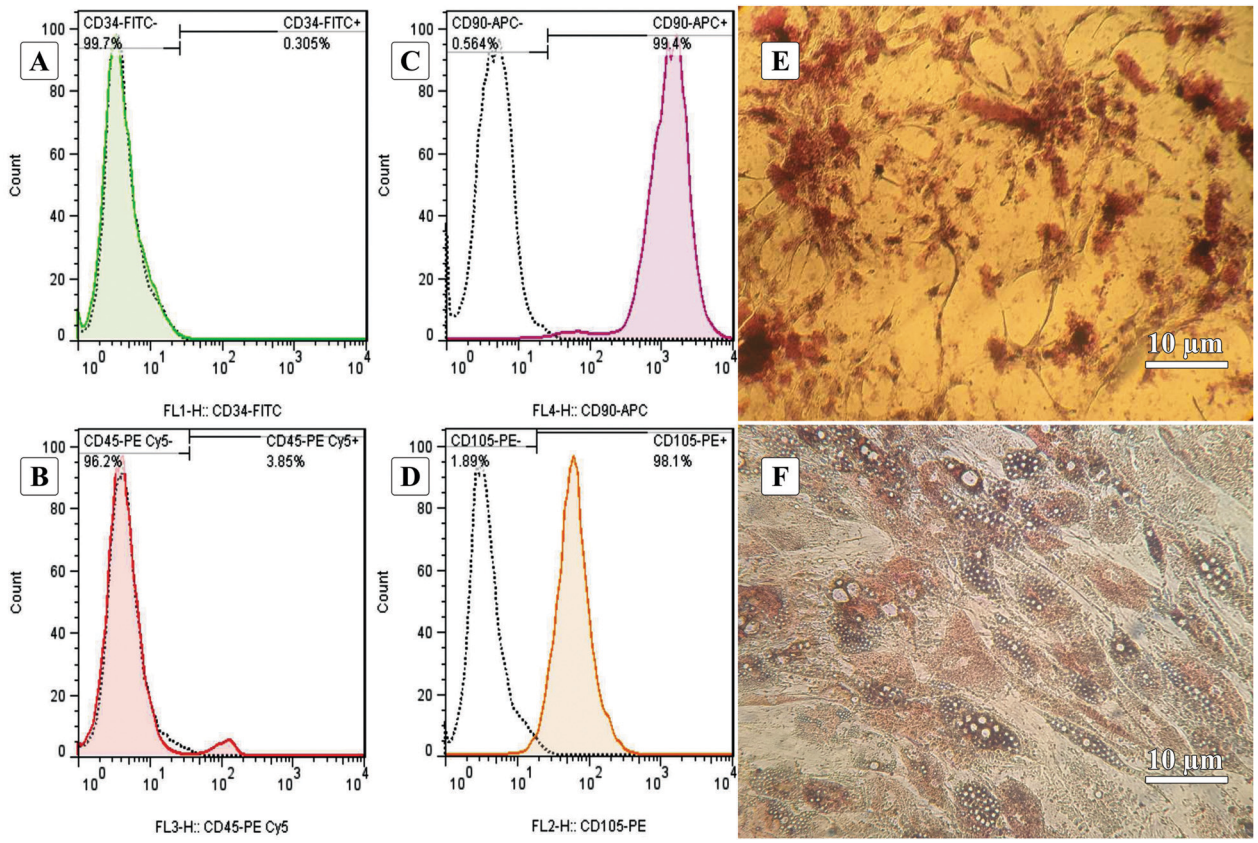

Fig. 1 Characterization of freshly isolated adipose-derived stem cells (ADSCs) by flow cytometry with negative and positive CD markers (a: CD34, b: CD45, c: CD90, and d: CD105). The dotted black lines are attributed to isotype controls. (e) Alizarin Red S staining of calcium depositions after osteogenic differentiation of ADSCs. (f) Oil Red O staining of adipogenic differentiation of ADSCs as evidenced by the formation of lipid droplets.

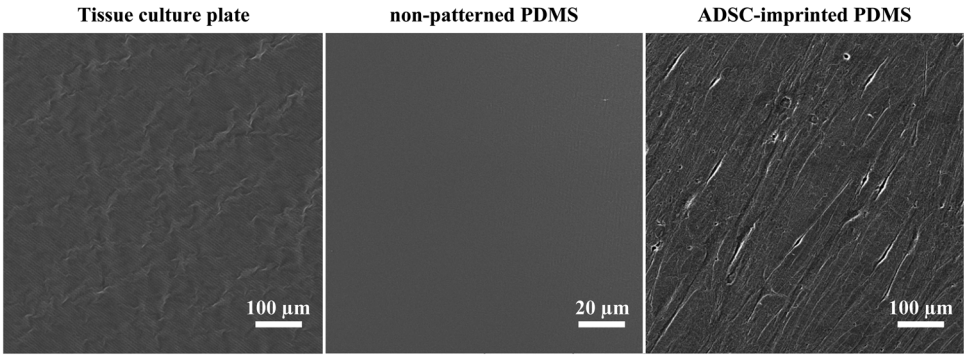

Fig. 2 Scanning electron micrographs of tissue culture polystyrene plate (TCP)-imprinted PDMS, PDMS with no imprint (air surface), and ADSC-imprinted PDMS.

replicas of different cells, the PDMS-based imprinting method assures a high-quality mold surface by replicating a surface roughness of less than 2 nm.[49] Also, Kamgouyan and coworkers fabricated substrates with the imprinted patterns of five spindle-like cell types and compared their nanotopography. They analyzed the substrates by AFM, obtained roughness profiles at the nanoscale, and confirmed the difference between the nanotopographies of the cellular imprints.[65] These findings can guarantee the usage of the PDMS imprinting method to copy and save the molecular pattern of the cell membrane precisely for future clinical regulation of cell behaviors.

Studies have shown that surface-specific nanotopograpies can affect the cell fate.[17,34] Cells respond to nanoscale surface features by actin- and fibril-based filopodia, by which cells explore the surface and understand it. Although the morphology of ADSCs at the micro-scale is similar to some primary cells such as osteoblasts, microscopic characteristics cannot solely stimulate the cells to exhibit a specific behavior.[53] Since cell-

imprinted substrates can mimic the nanoscale properties, cell templates are promising for cell culture applications.

3.3. Evaluation of adhesion and morphology of ADSCs

3.3.1. Effect of ADSC-imprinted substrates on the adhesion and proliferation of mesenchymal stem cells. Focal adhesion has been considered the starting point of cell-substrate interactions,[66] and plays a crucial role in subsequent cellular functions such as cell growth, proliferation, migration, and differentiation.[67] Physical and chemical cues such as topography, stiffness, and material properties can control adhesion and alter biochemical signaling.[66] Also, the tension between the substrate and cell membrane caused by adhesion can be effective in processes such as viability, proliferation, and differentiation of stem cells. Accordingly, the effect of ADSC patterns on cell adhesion and proliferation was investigated after seven days. ADSCs had high attachment and elongation on the TCP surface (Fig. 3), which could be due to the stiffness of TCP[66] (3 GPa[68]) and better adhesion conditions. ADSCs on non-patterned PDMS ($ADSC_P$ sample) had poor adhesion and spherical shape in aggregated colonies because of the inherent hydrophobicity of PDMS and its low stiffness. However, ADSCs cultured on the cell-imprinted PDMS surface ($ADSC_I$ sample) had an expected spindle shape for these cells. Despite the inherent hydrophobicity and low stiffness of the PDMS surface, $ADSC_I$ had better cell adhesion compared to $ADSC_P$, which could be attributed to the presence of irregular nanotopographies; because the cells grew randomly after isolation and before the fixation stage, creating an irregular ADSC-specific pattern was inevitable.

Fig. 4 shows the effect of surface characteristics on cell proliferation after 1, 3, 7, and 14 days for ADSCs cultured on TCP ($ADSC_T$), non-patterned PDMS ($ADSC_P$), and cell-imprinted PDMS ($ADSC_I$). Over time, it was found that the number of cells attached to the surface increased significantly in each group, such that the proliferation percentage for $ADSC_T$, $ADSC_P$, and $ADSC_I$ increased by 141.4, 122.5, and 149.9%, respectively, after 14 days. Although a high proliferation percent on TCP was expected because of its favorable surface characteristics for cell adhesion and proliferation, the presence of the ADSC template

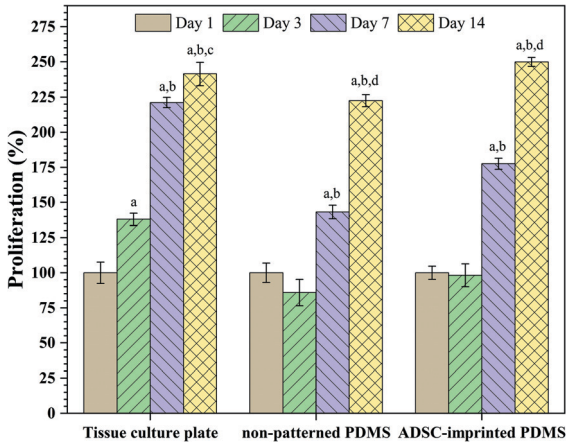

Fig. 4 Effect of cell adhesion on the proliferation of ADSCs cultured on the tissue culture plate, non-patterned PDMS, and ADSC-imprinted PDMS. ADSC stands for adipose-derived stem cell. Data show the means ± standard deviation. Different days in each sample were compared statistically by one-way ANOVA (a: $p < 0.0001$ day3-, day7-, day14-day1; b: $p < 0.0001$ day7-, day14-day3; c: $p < 0.05$ day7-day14; d: $p < 0.0001$ day7-day14).

in the $ADSC_I$ sample could largely eliminate the negative effect of the surface hydrophobicity of PDMS, causing a significant increase in the proliferation percent by 12.3% compared to $ADSC_P$ ($p < 0.001$). Moderate proliferation on the surface of PDMS with an ADSC membrane pattern reflects a moderate adhesion state that can provide an ADSC mechanism for self-renewal, differentiation suppression, and long-term *in vitro* culture. Adhesion strength to culture substrate determines the cell fate, such that stronger adhesion leads the stem cell to hard tissue phenotypes and weaker adhesion causes differentiation into soft tissues. So, creating a moderate surface stiffness associated with physical anchoring sites through cell-specific patterns can provide suitable cell adhesion and proliferation.

3.3.2. The effect of ADSC-imprinted substrates on cell morphology after long-term culture. After eight weeks, the morphologies of ADSCs cultured on TCP ($ADSC_T$ sample), non-patterned PDMS ($ADSC_P$ sample), and cell-imprinted PDMS ($ADSC_I$ sample) were evaluated by optical and fluorescence

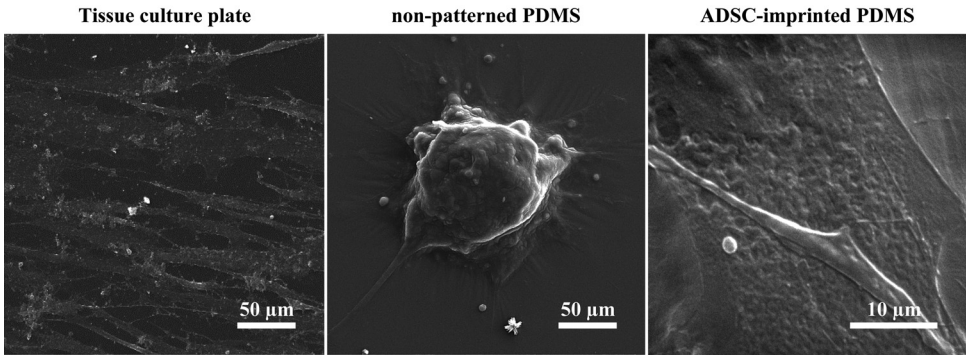

Fig. 3 Scanning electron micrographs of ADSCs cultured on TCP, non-patterned PDMS, and ADSC-imprinted substrate. ADSC stands for adipose-derived stem cell.

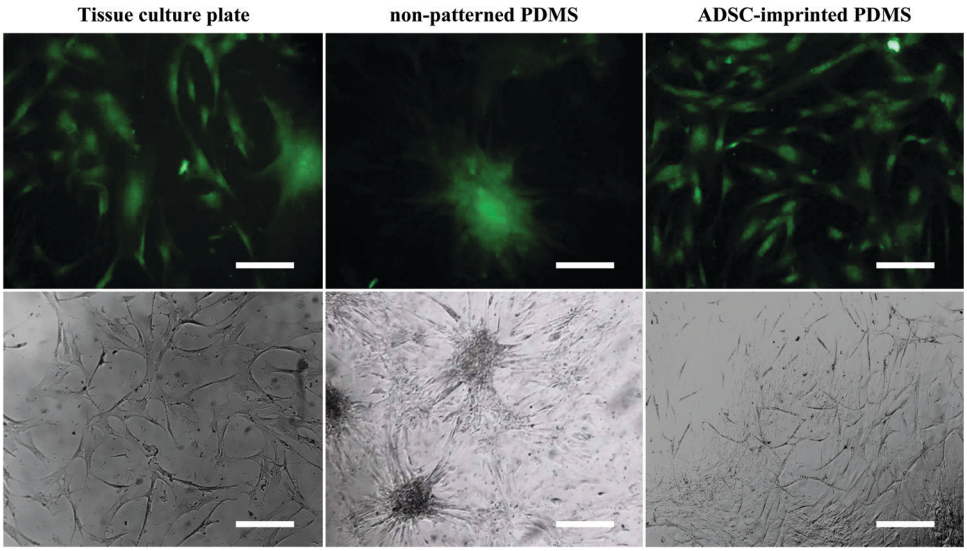

Fig. 5 Fluorescent (stained with DiI) and optical microscopic images of ADSCs cultured on different substrates (scale bar = 20 μm). ADSC stands for adipose-derive stem cell.

microscopy (Fig. 5). It can be observed that $ADSC_T$, having different polygonalized phenotypes and shapes, could spread and elongate on TCP. The $ADSC_P$ sample showed poor adhesion and aggregation, which was one of the main problems of using PDMS in stem cell culture. Because PDMS substrates had a lower cell, ADSCs were agglomerated and formed star-like shapes. On the contrary, the $ADSC_I$ sample could save the original spindle-like morphology, which could be attributed to the mimicry of cell shape at the micro- and nanoscale by maintaining the shape and position of the nucleus and cytoskeleton.

3.4. Cell population doubling time and cell cycle evaluation

Isolated ADSCs were subcultured every seven days up to 21 days on the surface of TCP ($ADSC_T$ sample), non-patterned PDMS ($ADSC_P$ sample), and ADSC-imprinted PDMS substrate ($ADSC_I$ sample) and counted at the end of each time point (passages 5, 6, and 7) to calculate cell population doubling time (CPDT). At passage 5, the CPDT of $ADSC_P$ and $ADSC_I$ was significantly lower than that of $ADSC_T$ by 24.2 and 28.5%, respectively (Fig. 6A). Despite similar reduction trends in CPDTs of $ADSC_P$ and $ADSC_I$ at passage 6, the presence of the ADSC pattern had a more significant effect on CPDT reduction ($p < 0.01$, 109%) compared to $ADSC_P$ (29.7%). Although CPDT of $ADSC_I$ did not change at passage 6 and significantly decreased at passage 7 ($p < 0.05$), CPDTs of $ADSC_T$ and $ADSC_P$ increased significantly at passage 6 ($p < 0.0001$ and $p < 0.01$ for $ADSC_T$ and $ADSC_P$, respectively), and decreased significantly at passage 7 for $ADSC_P$ ($p < 0.001$). At passage 7, the CPDTs of $ADSC_P$ and $ADSC_I$ were significantly lower than that of $ADSC_T$ by 45 and 61.2%, respectively. Despite the non-significant difference between the CPDTs of PDMS-based substrates, the presence of an ADSC pattern caused 30% in the CPDT compared to non-patterned PDMS ($ADSC_P$ sample).

Evaluation of the cell cycle at passage 8 showed that the number of ADSCs for the $ADSC_I$ sample in the S and G2/M phases increased more significantly than those of $ADSC_T$ and $ADSC_P$ samples (102.5 and 119.9% in the S phase, 96.6 and 118.9% in the G2/M phase) (Fig. 6B and Fig. S1, ESI†). In addition, a decreased G1 phase in the $ADSC_I$ sample compared to $ADSC_T$ and $ADSC_P$ samples (by 310 and 132%, respectively) was parallel to the decrease in doubling time and proved the prevention of ADSC differentiation.

Mesenchymal stem cells are in the stationary phase in tissue homeostatic conditions to protect against DNA damage. These cells are thought to become a functional phenotype for responding to tissue demands by producing rapidly proliferating progenitor cells before entering the area needing regeneration.[66] When mesenchymal stem cells are isolated from their native microenvironment *in vitro*, they enter an active form whose imprinted patterns save the features of that form at the micro- and nanoscale. So, the cell population rate increases, and the G1 phase decreases.

3.5. Effect of ADSC-imprinted substrates on ADSC stemness

3.5.1. Differentiation behavior of ADSCs cultured in adipogenic and osteogenic differentiating mediums. ADSCs were cultured in osteogenic, adipogenic, and complete cell culture mediums on the tissue culture plate ($ADSC_T$ sample), non-patterned PDMS ($ADSC_P$ sample), and ADSC-imprinted PDMS ($ADSC_I$ sample) for 21 days. Then cells were stained with Alizarin Red S and Oil Red O to assess osteogenic and adipogenic differentiation (Fig. 7).

$ADSC_T$ cultured in the osteogenic and adipogenic medium was differentiated into osteocyte- and adipocyte-like cells indicated by calcium precipitation and lipid droplet formation, respectively. Also, a little calcium precipitation was observed for $ADSC_T$ cultured in DMEM, which could be because of the TCP stiffness effect on stem cells.

$ADSC_P$ cultured in differentiating mediums showed osteogenic and adipogenic differentiation. However, $ADSC_P$ in adipogenic

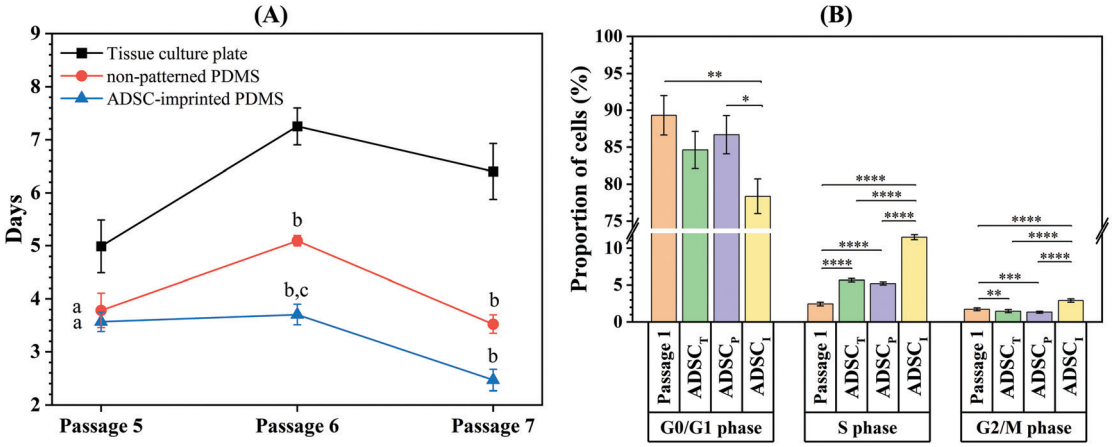

Fig. 6 (a) Cell population doubling time at various passages. Data show the means ± standard deviation. Different groups at each passage were compared statistically by one-way ANOVA (a: $p < 0.01$ compared to tissue culture plate, b: $p < 0.0001$ compared to tissue culture plate, c: $p < 0.01$ compared to non-patterned pdms). (b) Cell cycle phases in ADSCs cultured in different conditions. ADSC$_T$: ADSC on the tissue culture plate, ADSC$_P$: ADSC on non-patterned PDMS, ADSC$_I$: ADSC on ADSC-imprinted PDMS. ADSC stands for adipose-derive stem cell (*$p < 0.05$, **$p < 0.01$, *** $p < 0.001$, ****$p < 0.0001$).

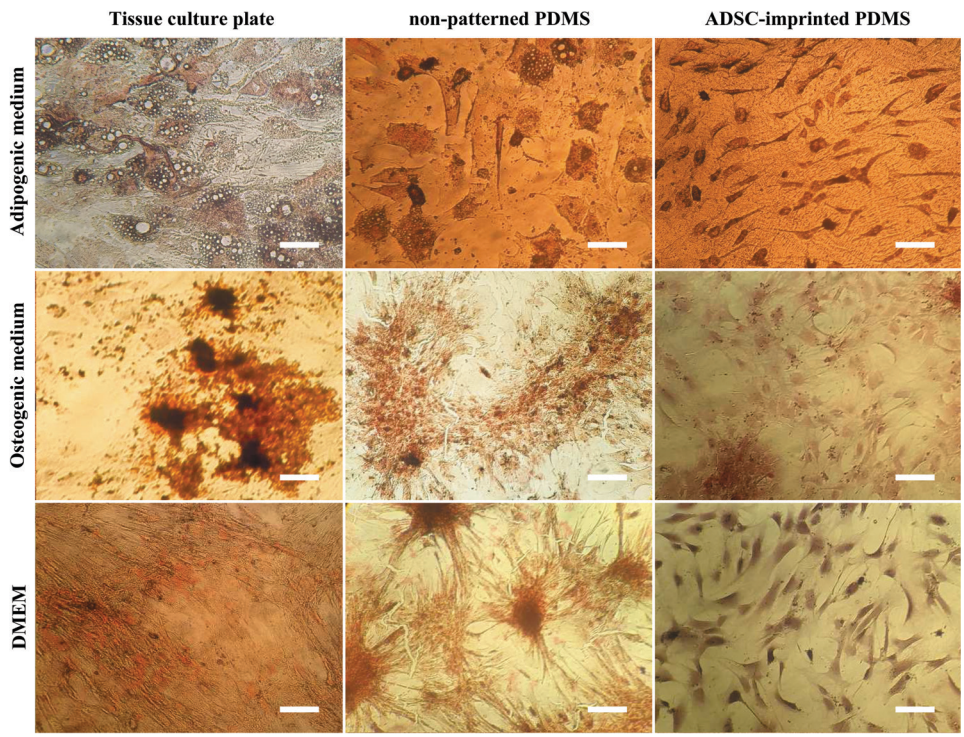

Fig. 7 ADSCs cultured on different substrates under adipogenic, osteogenic, and normal culture mediums, stained with Oil Red O and Alizarin Red S after 21 days. ADSC stands for adipose-derived stem cell (scale bar = 10 μm).

medium had spherical morphology due to the hydrophobicity and weak surface adhesion of non-patterned PDMS. By culturing in DMEM, calcium precipitation increased for ADSC$_P$, which might be because of the pressure between cellular aggregates and changes in gene expression.

However, the staining of ADSC$_I$ cultured in osteogenic and adipogenic medium revealed that ADSCs received the least differentiating effects from the mediums, resulting in low calcium deposition and rare lipid droplets. Furthermore, ADSC$_I$ could maintain its spindle-shaped morphology compared to ADSC$_P$, which had spherical morphology. Since it has been reported that the surface topography of a culture substrate can even maintain stem cells' stemness,[69] ADSC-specific surface topography can significantly reduce the influence of the differentiating mediums and maintain the stemness of stem cells for a long time.

3.5.2. Evaluation of specific surface markers after long-term cell culture. To evaluate long-term maintenance of stemness, ADSCs were cultured in DMEM for eight weeks on a tissue culture plate ($ADSC_T$), non-patterned PDMS ($ADSC_P$), and ADSC-imprinted PDMS ($ADSC_I$). Analyzing specific surface markers (Fig. 8 and Fig. S2 and S3, ESI†) confirmed unchanged CD90 expression for all substrates. However, the expression of the CD105 marker in $ADSC_I$ was more than those of $ADSC_T$ and $ADSC_P$.

To better understand the effect of ADSC-imprinting on ADSC fate, the cells were cultured in the adipogenic differentiating medium for 21 days. As can be seen in Fig. 8, the expression of CD105 marker $ADSC_I$ increased compared to the other two groups, though CD90 expression did not show a significant difference between all groups.

3.5.3. Gene expression analysis after long-term cell culture. Expression of specific surface markers (CD105, CD90, and CD34) and genes involved in osteogenesis (Col1A1 and OCN) and adipogenesis (PPRγ) pathways were analyzed by qPCR after eight weeks for ADSCs cultured on a tissue culture plate ($ADSC_T$), non-patterned PDMS ($ADSC_P$), and ADSC-imprinted PDMS ($ADSC_I$). Contrary to the nearly constant expression of the CD90 marker confirmed by flow cytometry (Fig. 8), qPCR results (Fig. 9) showed that CD90 and CD105 expressions for $ADSC_P$ and $ADSC_I$ were significantly higher than that of $ADSC_T$ ($p < 0.05$, ~19 and 28 times, respectively). Despite the non-significant reduction in expression of the CD105 marker in $ADSC_I$ (~18%) compared to $ADSC_P$, the presence of the ADSC template in $ADSC_I$ could improve its CD90 expression significantly ($p < 0.05$) by 43%.

Although expressions of CD34 (as a negative marker for ADSC) in $ADSC_I$ and particularly in $ADSC_P$ were significantly higher than that of $ADSC_T$, the fold change of CD34 for $ADSC_I$ was 2.36 times greater than $ADSC_T$ only. Furthermore, the influence of the ADSC template ($ADSC_I$ sample) on CD34 downregulation by ~87% was significant ($p < 0.05$) compared to $ADSC_P$, proving the more positive effect of the ADSC template on stemness maintenance.

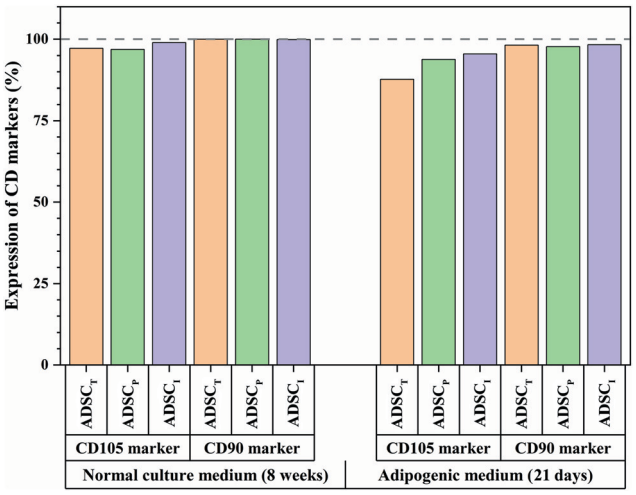

Fig. 8 Flow cytometry results for CD105 and CD90 markers of ADSCs cultured on different substrates for 8 weeks in DMEM and 21 days in adipogenic medium. $ADSC_T$: ADSC on the tissue culture plate, $ADSC_P$: ADSC on non-patterned PDMS, $ADSC_I$: ADSC on ADSC-imprinted PDMS. ADSC stands for adipose-derived stem cell.

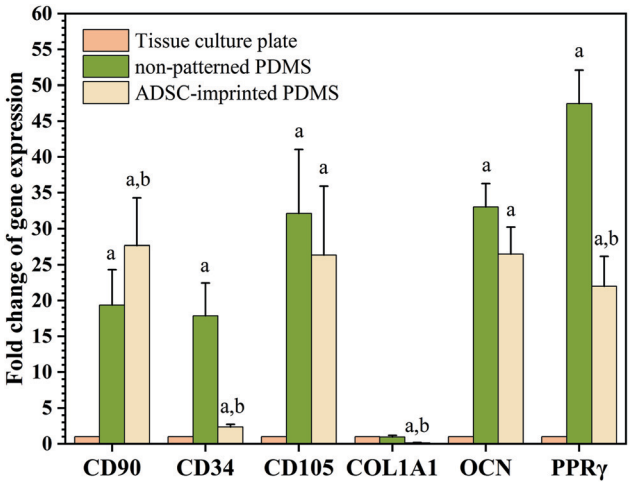

Fig. 9 Real time-PCR (QPCR) results of ADSCs cultured on different substrates after 8 passages for different markers. Data show the means ± standard deviation. Different groups were compared statistically by one-way ANOVA (a: $p < 0.05$ compared to tissue culture plate, b: $p < 0.05$ compared to non-patterned PDMS).

The PPRγ analysis demonstrated significant upregulation in $ADSC_P$ and $ADSC_I$ compared to $ADSC_T$, which was inevitable due to the effect of lower surface stiffness on adipogenic differentiation. Also, the lower strength of cell adhesion can promote the expression of adipocyte-specific genes.[66] Although $ADSC_P$ and $ADSC_I$ had similar surface stiffness because of the same chemical composition and fabrication process, the presence of an ADSC-specific template in the $ADSC_I$ sample could decrease PPRγ expression by ~53.7% supporting the exact application of ADSC-imprinting to produce a better cell culture substrate. Various studies have shown that increasing the expression of CD90 reduces the ability of stem cells to differentiate into adipose cells.[70,71] Therefore, the presence of an ADSC-specific pattern could protect ADSCs against adipogenesis, thereby maintaining stemness long-term.

Analysis of specific genes involved in the osteogenesis pathway showed that Col1A1 underwent significant downregulation in $ADSC_I$ compared to $ADSC_T$ and $ADSC_P$ (by ~85% for both samples), confirming the positive effect of the ADSC template on protecting ADSCs against osteogenic differentiation. Although the OCN gene was significantly upregulated in $ADSC_P$ and $ADSC_I$ compared to $ADSC_T$, the positive presence of the ADSC template caused a ~20% decrease in OCN level compared to $ADSC_P$.

The qPCR results were truly conformed to Alizarin Red S and Oil Red O staining of ADSCs cultured on different substrates under osteogenic and adipogenic conditions (Fig. 7). Despite higher cytoplasmic expression of some osteogenic and adipogenic genes in PDMS-based substrates, other results demonstrating morphological or functional characteristics (microscopic imaging, staining, and flow cytometry) confirmed that PDMS-based

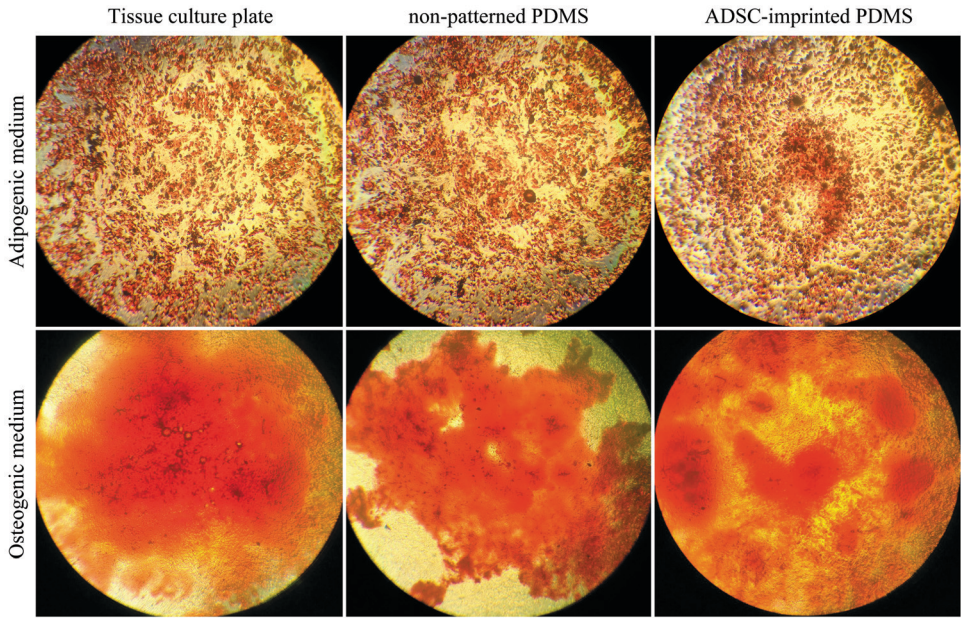

Fig. 10 Multipotential ability of ADSCs cultured on different substrates for eight weeks, exposed to adipogenic and osteogenic mediums, stained with Oil Red O and Alizarin Red S after 21 days. ADSC stands for adipose-derived stem cell.

substrates, particularly ADSC-imprinted ones, did not follow differentiation pathways, and the ADSC-specific pattern had a noteworthy influence on long-term stemness maintenance.

3.5.4. Multipotency evaluation after long-term cell culturing. To confirm the differentiation capacity of ADSCs cultured on different substrates for eight weeks, they were exposed to adipogenic and osteogenic mediums for 21 days and stained by Alizarin Red S and Oil Red O. Fig. 10 shows that three ADSC populations obtained from TCP ($ADSC_T$ sample), non-patterned PDMS ($ADSC_P$ sample), and ADSC-imprinted PDMS ($ADSC_I$ sample) had adipogenic and osteogenic potential. However, adipogenesis in $ADSC_P$ was seemingly higher than in $ADSC_I$, which might be attributed to higher PPRγ expression due to a lower strength of cell adhesion; it might be deduced that $ADSC_P$ began to follow the adipogenesis pathway resulting in better adipogenic differentiation. Nevertheless, the $ADSC_I$ was quite successful in adipogenic differentiation and was able to produce many lipid droplets. In the case of osteogenesis, all samples were successful and could form calcium deposits on almost the entire surface of the plate.

Examination of several commercial TCPs has shown that their surface topography is different (ranged 1–7 nm), resulting in various protein adsorption and population doubling.[72] Also, spontaneous differentiation of MSCs by culturing them on common TCP causes rapid diminution resulting in a heterogeneous population of predominantly fibroblastic phenotype.[73] Although the differentiation potential of TCP and ADSC-imprinted PDMS has similarities to some extent, it is probable that using commercial TCPs in each clinical center and the possibility of changes in laboratory equipment may cause heterogeneous consequences for clinical therapies. So, creating a culture substrate having cell-specific, cell-friendly, and maybe reproducible patterns can increase success in cell-based studies and therapies.

4. Conclusions

The application of stem cells to heal various diseases has received more attention in the last few decades. To control the differentiation of stem cells and form a homogeneous population *in vitro*, biomaterial–cell interactions and making a substrate that can control cellular functions without using chemical agents have become an interesting topic recently. However, the produced substrate should have features such as easy fabrication, cheapness, large-scale production, easy use for different users, and availability of raw materials and equipment.

Although common tissue culture plates (TCPs) can be used for many stem cell applications, it is expected that using commercial TCPs may cause heterogeneous consequences for clinical therapies throughout the world because of their variety of surface topography. So, creating a culture substrate with a cell-friendly pattern can ensure success in cell-based studies and therapies. Cell-imprinted substrates can also be autoclaved for multiple usages, which reduces costs and creates appropriate maintenance conditions for *in vitro* cell culture.

In this study, we discussed a novel approach to making a suitable culture substrate for the long-term expansion of stem cells. We isolated adipose-derived stem cells (ADSCs), developed a PDMS-based substrate having an ADSC-specific pattern and performed some evaluations to analyze the capability of the ADSC-imprinted PDMS substrate to delay cell differentiation and maintain stemness after long-term cell culture. In comparison to

common TCP and non-patterned PDMS, ADSC-imprinted PDMS had better cell attachment and the highest proliferation percentage due to the presence of ADSC patterns. It could capture the ADSCs' topography well and stimulate cultured ADSCs to present their original spindle-like morphology compared to other substrates. The presence of an ADSC-specific pattern significantly decreased the cell population doubling time compared to TCP and influenced phases of the cell cycle, resulting in more rapid cell division. Furthermore, the ADSC-specific pattern could largely prevent the differentiation of ADSCs cultured on the substrate, confirming the positive effect of specific surface topography on stemness maintenance. After long-term cell culturing, ADSC-specific surface markers were highly expressed on the cell membrane underlying stemness preservation. It can be concluded that biomimetic ADSC-imprinted substrates delay stem cell differentiation *in vitro* while maintaining their proliferative potential even when differentiating stimulations are used.

Conflicts of interest

There are no conflicts to declare.

Acknowledgements

This work was supported by the Pasteur Institute of Iran [grant no. 1707]; and Iran Food and Drug Administration (IFDA) [grant no. Pr977302].

References

1 S. Lopa, C. Mondadori, V. L. Mainardi, G. Talò, M. Costantini, C. Candrian, W. Swieszkowski and M. Moretti, Translational application of microfluidics and bioprinting for stem cell-based cartilage repair, *Stem Cells Int.*, 2018, **2018**, 6594841, DOI: **10.1155/2018/6594841**.

2 S. Yazdian Kashani, M. Keshavarz Moraveji, M. Taghipoor, R. Kowsari-Esfahan, A. A. Hosseini, L. Montazeri, M. M. Dehghan, H. Gholami, S. Farzad-Mohajeri, M. Mehrjoo, M. Majidi, P. Renaud and S. Bonakdar, An integrated microfluidic device for stem cell differentiation based on cell-imprinted substrate designed for cartilage regeneration in a rabbit model, *Mater. Sci. Eng., C*, 2021, **121**, 111794, DOI: **10.1016/j.msec.2020.111794**.

3 Y. Liu, G. Zhou and Y. Cao, Recent Progress in Cartilage Tissue Engineering—Our Experience and Future Directions, *Engineering*, 2017, **3**, 28–35, DOI: **10.1016/J.ENG.2017.01.010**.

4 M. Mohammed, T. S. Lai and H. C. Lin, Substrate stiffness and sequence dependent bioactive peptide hydrogels influence the chondrogenic differentiation of human mesenchymal stem cells, *J. Mater. Chem. B*, 2021, **9**, 1676–1685, DOI: **10.1039/d0tb02008g**.

5 Y. H. K. Yang, C. R. Ogando, C. Wang See, T. Y. Chang and G. A. Barabino, Changes in phenotype and differentiation potential of human mesenchymal stem cells aging *in vitro*, *Stem Cell Res. Ther.*, 2018, **9**, 1–14, DOI: **10.1186/s13287-018-0876-3**.

6 C. Li, H. Zhao, L. Cheng and B. Wang, Allogeneic *vs.* autologous mesenchymal stem/stromal cells in their medication practice, *Cell Biosci.*, 2021, **11**, 1–21, DOI: **10.1186/s13578-021-00698-y**.

7 W. Zakrzewski, M. Dobrzyński, M. Szymonowicz and Z. Rybak, Stem cells: Past, present, and future, *Stem Cell Res. Ther.*, 2019, **10**, 68, DOI: **10.1186/s13287-019-1165-5**.

8 M. Kabat, I. Bobkov, S. Kumar and M. Grumet, Trends in mesenchymal stem cell clinical trials 2004-2018: Is efficacy optimal in a narrow dose range, *Stem Cells Transl. Med.*, 2020, **9**, 17–27, DOI: **10.1002/sctm.19-0202**.

9 S. K. Kureel, P. Mogha, A. Khadpekar, V. Kumar, R. Joshi, S. Das, J. Bellare and A. Majumder, Soft substrate maintains proliferative and adipogenic differentiation potential of human mesenchymal stem cells on long-term expansion by delaying senescence, *Biol. Open*, 2019, **8**(4), bio039453, DOI: **10.1242/bio.039453**.

10 I. Jun, H. S. Han, J. W. Lee, K. Lee, Y. C. Kim, M. R. Ok, H. K. Seok, Y. J. Kim, I. S. Song, H. Shin, J. R. Edwards, K. Y. Lee and H. Jeon, On/off switchable physical stimuli regulate the future direction of adherent cellular fate, *J. Mater. Chem. B*, 2021, **9**, 5560–5571, DOI: **10.1039/d1tb00908g**.

11 K. Ishihara, M. Kaneyasu, K. Fukazawa, R. Zhang and Y. Teramura, Induction of mesenchymal stem cell differentiation by co-culturing with mature cells in double-layered 2-methacryloyloxyethyl phosphorylcholine polymer hydrogel matrices, *J. Mater. Chem. B*, 2022, **10**, 2561–2569, DOI: **10.1039/d1tb01817e**.

12 F. Etezadi, M. N. T. Le, H. Shahsavarani, A. Alipour, N. Moazzezy, S. Samani, A. Amanzadeh, S. Pahlavan, S. Bonakdar, M. A. Shokrgozar and K. Hasegawa, Optimization of a PDMS-Based Cell Culture Substrate for High-Density Human-Induced Pluripotent Stem Cell Adhesion and Long-Term Differentiation into Cardiomyocytes under a Xeno-Free Condition, *ACS Biomater. Sci. Eng.*, 2022, **8**(5), 2040–2052, DOI: **10.1021/acsbiomaterials.2c00162**.

13 F. Han, C. Zhu, Q. Guo, H. Yang and B. Li, Cellular modulation by the elasticity of biomaterials, *J. Mater. Chem. B*, 2016, **4**, 9–26, DOI: **10.1039/c5tb02077h**.

14 E. S. Place, N. D. Evans and M. M. Stevens, Complexity in biomaterials for tissue engineering, *Nat. Mater.*, 2009, **8**, 457–470, DOI: **10.1038/nmat2441**.

15 C. Y. Yang, W. Y. Huang, L. H. Chen, N. W. Liang, H. C. Wang, J. Lu, X. Wang and T. W. Wang, Neural tissue engineering: The influence of scaffold surface topography and extracellular matrix microenvironment, *J. Mater. Chem. B*, 2021, **9**, 567–584, DOI: **10.1039/d0tb01605e**.

16 A. Steier, A. Muñiz, D. Neale and J. Lahann, Emerging Trends in Information-Driven Engineering of Complex Biological Systems, *Adv. Mater.*, 2019, **31**(26), DOI: **10.1002/adma.201806898**.

17 A. Higuchi, Q. D. Ling, S. S. Kumar, Y. Chang, A. A. Alarfaj, M. A. Munusamy, K. Murugan, S. T. Hsu and A. Umezawa, Physical cues of cell culture materials lead the direction of

differentiation lineages of pluripotent stem cells, *J. Mater. Chem. B*, 2015, **3**, 8032–8058, DOI: 10.1039/c5tb01276g.

18 K. Metavarayuth, E. Villarreal, H. Wang and Q. Wang, Surface topography and free energy regulate osteogenesis of stem cells: effects of shape-controlled gold nanoparticles, *Biomater. Transl.*, 2021, **2**, 165–173, DOI: 10.12336/biomatertransl.2021.02.006.

19 L. Jia, F. Han, H. Wang, C. Zhu, Q. Guo, J. Li, Z. Zhao, Q. Zhang, X. Zhu and B. Li, Polydopamine-assisted surface modification for orthopaedic implants, *J. Orthop. Transl.*, 2019, **17**, 82–95, DOI: 10.1016/j.jot.2019.04.001.

20 R. S. Fischer, K. A. Myers, M. L. Gardel and C. M. Waterman, Stiffness-controlled three-dimensional extracellular matrices for high-resolution imaging of cell behavior, *Nat. Protoc.*, 2012, **7**, 2056–2066, DOI: 10.1038/nprot.2012.127.

21 W. Wang, H. Cui, P. Zhang, J. Meng, F. Zhang and S. Wang, Efficient Capture of Cancer Cells by Their Replicated Surfaces Reveals Multiscale Topographic Interactions Coupled with Molecular Recognition, *ACS Appl. Mater. Interfaces*, 2017, **9**, 10537–10543, DOI: 10.1021/acsami.7b01147.

22 X. Zhou, J. Shi, F. Zhang, J. Hu, X. Li, L. Wang, X. Ma and Y. Chen, Reversed cell imprinting, AFM imaging and adhesion analyses of cells on patterned surfaces, *Lab Chip*, 2010, **10**, 1182–1188, DOI: 10.1039/b926325j.

23 L. Yang, L. Yang, L. Ge, L. Ge, P. Van Rijn and P. Van Rijn, Synergistic Effect of Cell-Derived Extracellular Matrices and Topography on Osteogenesis of Mesenchymal Stem Cells, *ACS Appl. Mater. Interfaces*, 2020, **12**, 25591–25603, DOI: 10.1021/acsami.0c05012.

24 D. Hernandez, E. T. Ritschdorff, J. L. Connell and J. B. Shear, In Situ Imprinting of Topographic Landscapes at the Cell-Substrate Interface, *J. Am. Chem. Soc.*, 2018, **140**, 14064–14068, DOI: 10.1021/jacs.8b09226.

25 S. Kumari, S. Vermeulen, B. Van Der Veer, A. Carlier, J. De Boer and D. Subramanyam, Shaping Cell Fate: Influence of Topographical Substratum Properties on Embryonic Stem Cells, *Tissue Eng., Part B*, 2018, **24**, 255–266, DOI: 10.1089/ten.teb.2017.0468.

26 P. Bhattacharjee, B. L. Cavanagh and M. Ahearne, Effect of substrate topography on the regulation of human corneal stromal cells, *Colloids Surf., B*, 2020, **190**, 110971, DOI: 10.1016/j.colsurfb.2020.110971.

27 B. Bellei, E. Migliano, M. Tedesco, S. Caputo, F. Papaccio, G. Lopez and M. Picardo, Adipose tissue-derived extracellular fraction characterization: Biological and clinical considerations in regenerative medicine, *Stem Cell Res. Ther.*, 2018, **9**, 1–18, DOI: 10.1186/s13287-018-0956-4.

28 J. Liu, Y. Ding, Z. Liu and X. Liang, Senescence in Mesenchymal Stem Cells: Functional Alterations, Molecular Mechanisms, and Rejuvenation Strategies, *Front. Cell Dev. Biol.*, 2020, **8**, 258, DOI: 10.3389/fcell.2020.00258.

29 P. P. S. S. Abadi, J. C. Garbern, S. Behzadi, M. J. Hill, J. S. Tresback, T. Heydari, M. R. Ejtehadi, N. Ahmed, E. Copley, H. Aghaverdi, R. T. Lee, O. C. Farokhzad and M. Mahmoudi, Engineering of Mature Human Induced Pluripotent Stem Cell-Derived Cardiomyocytes Using Substrates with Multiscale Topography, *Adv. Funct. Mater.*, 2018, **28**, 1707378, DOI: 10.1002/adfm.201707378.

30 G. Abagnale, A. Sechi, M. Steger, Q. Zhou, C. C. Kuo, G. Aydin, C. Schalla, G. Müller-Newen, M. Zenke, I. G. Costa, P. van Rijn, A. Gillner and W. Wagner, Surface Topography Guides Morphology and Spatial Patterning of Induced Pluripotent Stem Cell Colonies, *Stem Cell Rep.*, 2017, **9**, 654–666, DOI: 10.1016/j.stemcr.2017.06.016.

31 M. Ali and J. B. Shear, Real time remodeling of cellular morphology using optical imprinting of cell-culture substrates, *Biomed. Phys. Eng. Express*, 2019, **5**, 035029, DOI: 10.1088/2057-1976/aafc8e.

32 E. Costa, C. González-García, J. L. Gómez Ribelles and M. Salmerón-Sánchez, Maintenance of chondrocyte phenotype during expansion on PLLA microtopographies, *J. Tissue Eng.*, 2018, **9**, 1–10, DOI: 10.1177/2041731418789829.

33 B. Liu, C. Tao, Z. Wu, H. Yao and D.-A. Wang, Engineering strategies to achieve efficient *in vitro* expansion of haematopoietic stem cells: development and improvement, *J. Mater. Chem. B*, 2022, **10**, 1734–1753, DOI: 10.1039/d1tb02706a.

34 J. O. Abaricia, N. Farzad, T. J. Heath, J. Simmons, L. Morandini and R. Olivares-Navarrete, Control of innate immune response by biomaterial surface topography, energy, and stiffness, *Acta Biomater.*, 2021, **133**, 58–73, DOI: 10.1016/j.actbio.2021.04.021.

35 A. J. Engler, S. Sen, H. L. Sweeney and D. E. Discher, Matrix Elasticity Directs Stem Cell Lineage Specification, *Cell*, 2006, **126**, 677–689, DOI: 10.1016/j.cell.2006.06.044.

36 A. F. Bonatti, C. De Maria and G. Vozzi, Molecular imprinting strategies for tissue engineering applications: A review, *Polymers*, 2021, **13**, 1–20, DOI: 10.3390/polym13040548.

37 K. Zhang, X. Xiao, X. Wang, Y. Fan and X. Li, Topographical patterning: Characteristics of current processing techniques, controllable effects on material properties and co-cultured cell fate, updated applications in tissue engineering, and improvement strategies, *J. Mater. Chem. B*, 2019, **7**, 7090–7109, DOI: 10.1039/c9tb01682a.

38 W. Zhao, B. Li, S. Xu, X. Huang, J. Luo, Y. Zhu and X. Liu, Electrochemical protein recognition based on macromolecular self-assembly of molecularly imprinted polymer: A new strategy to mimic antibody for label-free biosensing, *J. Mater. Chem. B*, 2019, **7**, 2311–2319, DOI: 10.1039/c9tb00220k.

39 A. K. Venkataraman, J. R. Clegg and N. A. Peppas, Polymer composition primarily determines the protein recognition characteristics of molecularly imprinted hydrogels, *J. Mater. Chem. B*, 2020, **8**, 7685–7695, DOI: 10.1039/d0tb01627f.

40 M. Komiyama, T. Mori and K. Ariga, Molecular imprinting: materials nanoarchitectonics with molecular information, *Bull. Chem. Soc. Jpn.*, 2018, **91**, 1075–1111.

41 T. Saeki, E. Takano, H. Sunayama, Y. Kamon, R. Horikawa, Y. Kitayama and T. Takeuchi, Signalling molecular recognition nanocavities with multiple functional groups prepared by molecular imprinting and sequential post-imprinting modifications for prostate cancer biomarker glycoprotein detection, *J. Mater. Chem. B*, 2020, **8**, 7987–7993, DOI: 10.1039/d0tb00685h.

42 S. Yazdian Kashani, A. Afzalian, F. Shirinichi and M. Keshavarz Moraveji, Microfluidics for core–shell drug carrier particles – a review, *RSC Adv.*, 2020, **11**, 229–249, DOI: **10.1039/d0ra08607j**.

43 Y. Shao, J. M. Mann, W. Chen and J. Fu, Global architecture of the F-actin cytoskeleton regulates cell shape-dependent endothelial mechanotransduction, *Integr. Biol.*, 2014, **6**, 300–311, DOI: **10.1039/c3ib40223a**.

44 R. C. Lyon, F. Zanella, J. H. Omens and F. Sheikh, Mechanotransduction in cardiac hypertrophy and failure, *Circ. Res.*, 2015, **116**, 1462–1476, DOI: **10.1161/CIRCRESAHA.116.304937**.

45 M. Ehrbar, S. C. Rizzi, R. Hlushchuk, V. Djonov, A. H. Zisch, J. A. Hubbell, F. E. Weber and M. P. Lutolf, Enzymatic formation of modular cell-instructive fibrin analogs for tissue engineering, *Biomaterials*, 2007, **28**, 3856–3866, DOI: **10.1016/j.biomaterials.2007.03.027**.

46 H. Kavand, H. Van Lintel, S. Bakhshi Sichani, S. Bonakdar, H. Kavand, J. Koohsorkhi and P. Renaud, Cell-Imprint Surface Modification by Contact Photolithography-Based Approaches: Direct-Cell Photolithography and Optical Soft Lithography Using PDMS Cell Imprints, *ACS Appl. Mater. Interfaces*, 2019, **11**, 10559–10566, DOI: **10.1021/acsami.9b00523**.

47 S. Bonakdar, M. Mahmoudi, L. Montazeri, M. Taghipoor, A. Bertsch, M. A. Shokrgozar, S. Sharifi, M. Majidi, O. Mashinchian, M. H. Sekachaei, P. Zolfaghari and P. Renaud, Cell-Imprinted Substrates Modulate Differentiation, Redifferentiation, and Transdifferentiation, *ACS Appl. Mater. Interfaces*, 2016, **8**, 13777–13784, DOI: **10.1021/acsami.6b03302**.

48 O. Mashinchian, S. Bonakdar, H. Taghinejad, V. Satarifard, M. Heidari, M. Majidi, S. Sharifi, A. Peirovi, S. Saffar, M. Taghinejad, M. Abdolahad, S. Mohajerzadeh, M. A. Shokrgozar, S. M. Rezayat, M. R. Ejtehadi, M. J. Dalby and M. Mahmoudi, Cell-imprinted substrates act as an artificial niche for skin regeneration, *ACS Appl. Mater. Interfaces*, 2014, **6**, 13280–13292, DOI: **10.1021/am503045b**.

49 M. Mahmoudi, S. Bonakdar, M. A. Shokrgozar, H. Aghaverdi, R. Hartmann, A. Pick, G. Witte and W. J. Parak, Cell-imprinted substrates direct the fate of stem cells, *ACS Nano*, 2013, **7**, 8379–8384, DOI: **10.1021/nn403844q**.

50 M. T. Lam and M. T. Longaker, Comparison of several attachment methods for human iPS, embryonic and adipose-derived stem cells for tissue engineering, *J. Tissue Eng. Regen. Med.*, 2012, **6**, s80–s86, DOI: **10.1002/term.1499**.

51 J. N. Lee, X. Jiang, D. Ryan and G. M. Whitesides, Compatibility of mammalian cells on surfaces of poly(dimethylsiloxane), *Langmuir*, 2004, **20**, 11684–11691, DOI: **10.1021/la048562**.

52 J. Zhou, A. V. Ellis and N. H. Voelcker, Recent developments in PDMS surface modification for microfluidic devices, *Electrophoresis*, 2010, **31**, 2–16, DOI: **10.1002/elps.200900475**.

53 K. Kamguyan, A. A. Katbab, M. Mahmoudi, E. Thormann, S. Zajforoushan Moghaddam, L. Moradi and S. Bonakdar, An engineered cell-imprinted substrate directs osteogenic differentiation in stem cells, *Biomater. Sci.*, 2018, **6**, 189–199, DOI: **10.1039/c7bm00733g**.

54 Z. S. Ghazali, M. Eskandari, S. Bonakdar, P. Renaud, O. Mashinchian, S. Shalileh, F. Bonini, I. Uckay, O. Preynat-Seauve and T. Braschler, Neural priming of adipose-derived stem cells by cell-imprinted substrates, *Biofabrication*, 2021, **13**, 035009, DOI: **10.1088/1758-5090/abc66f**.

55 S. Dadashkhan, S. Irani, S. Bonakdar and B. Ghalandari, P75 and S100 gene expression induced by cell-imprinted substrate and beta-carotene to nerve tissue engineering, *J. Appl. Polym. Sci.*, 2021, **138**, 50624, DOI: **10.1002/app.50624**.

56 M. Moosazadeh Moghaddam, S. Bonakdar, M. A. Shokrgozar, A. Zaminy, H. Vali and S. Faghihi, Engineered substrates with imprinted cell-like topographies induce direct differentiation of adipose-derived mesenchymal stem cells into Schwann cells, *Artif. Cells, Nanomed., Biotechnol.*, 2019, **47**, 1022–1035, DOI: **10.1080/21691401.2019.1586718**.

57 S. M. A. Haramshahi, S. Bonakdar, M. Moghtadaei, K. Kamguyan, E. Thormann, S. Tanbakooei, S. Simorgh, P. Brouki-Milan, N. Amini, N. Latifi, M. T. Joghataei, A. Samadikuchaksaraei, M. Katebi and M. Soleimani, Tenocyte-imprinted substrate: A topography-based inducer for tenogenic differentiation in adipose tissue-derived mesenchymal stem cells, *Biomed. Mater.*, 2020, **15**, 035014, DOI: **10.1088/1748-605X/ab6709**.

58 J. Medlock, A. A. K. Das, L. A. Madden, D. J. Allsup and V. N. Paunov, Cancer bioimprinting and cell shape recognition for diagnosis and targeted treatment, *Chem. Soc. Rev.*, 2017, **46**, 5110–5127, DOI: **10.1039/c7cs00179g**.

59 S. Yazdian Kashani, M. Keshavarz Moraveji and S. Bonakdar, Computational and experimental studies of a cell-imprinted-based integrated microfluidic device for biomedical applications, *Sci. Rep.*, 2021, **11**, 1–17, DOI: **10.1038/s41598-021-91616-2**.

60 M. A. Shokrgozar, M. Fattahi, S. Bonakdar, I. R. Kashani, M. Majidi, N. Haghighipour, V. Bayati, H. Sanati and S. N. Saeedi, Healing potential of mesenchymal stem cells cultured on a collagen-based scaffold for skin regeneration, *Iran. Biomed. J.*, 2012, **16**, 1–9, DOI: **10.6091/ibj.1053.2012**.

61 H. Ghaneialvar, L. Soltani, H. R. Rahmani, A. S. Lotfi and M. Soleimani, Characterization and Classification of Mesenchymal Stem Cells in Several Species Using Surface Markers for Cell Therapy Purposes, *Indian J. Clin. Biochem.*, 2018, **33**, 46–52, DOI: **10.1007/s12291-017-0641-x**.

62 S. T. L. Pinto Filho, M. M. Pillat, M. P. Rosa, F. Dalmolin, H. Ulrich and N. L. Pippi, Expression patterns of mesenchymal stem cell-specific proteins in adipose tissue-derived cells: possible immunosuppressing agent in partial allograft for restoring the urinary bladder in rabbits, *Pesqui. Veterinária Bras.*, 2018, **38**, 2183–2189.

63 F. Aleahmad, S. Ebrahimi, M. Salmannezhad, M. Azarnia, M. Jaberipour, M. Hoseini and T. Talaei-Khozani, Heparin/Collagen 3D Scaffold Accelerates Hepatocyte Differentiation of Wharton's Jelly-Derived Mesenchymal, *Stem Cells, Tissue*

Eng. Regener. Med., 2017, **14**, 443–452, DOI: **10.1007/s13770-017-0048-z**.

64 L. R. Smith, S. Cho and D. E. Discher, Stem cell differentiation is regulated by extracellular matrix mechanics, *Physiology*, 2018, **33**, 16–25, DOI: **10.1152/physiol.00026.2017**.

65 K. Kamguyan, S. Z. Moghaddam, A. Nazbar, S. M. A. Haramshahi, S. Taheri, S. Bonakdar and E. Thormann, Cell-imprinted substrates: In search of nanotopographical fingerprints that guide stem cell differentiation, *Nanoscale Adv.*, 2021, **3**, 333–338, DOI: **10.1039/d0na00692k**.

66 M. J. Dalby, N. Gadegaard and R. O. C. Oreffo, Harnessing nanotopography and integrin-matrix interactions to influence stem cell fate, *Nat. Mater.*, 2014, **13**, 558–569, DOI: **10.1038/nmat3980**.

67 A. J. García, Get a grip: Integrins in cell-biomaterial interactions, *Biomaterials*, 2005, **26**, 7525–7529, DOI: **10.1016/j.biomaterials.2005.05.029**.

68 P. M. Gilbert, K. L. Havenstrite, K. E. G. Magnusson, A. Sacco, N. A. Leonardi, P. Kraft, N. K. Nguyen, S. Thrun, M. P. Lutolf and H. M. Blau, Substrate elasticity regulates skeletal muscle stem cell self-renewal in culture, *Science*, 2010, **329**, 1078–1081, DOI: **10.1126/science.1191035**.

69 M. J. Dalby, N. Gadegaard, R. Tare, A. Andar, M. O. Riehle, P. Herzyk, C. D. W. Wilkinson and R. O. C. Oreffo, The control of human mesenchymal cell differentiation using nanoscale symmetry and disorder, *Nat. Mater.*, 2007, **6**, 997–1003, DOI: **10.1038/nmat2013**.

70 C. F. Woeller, C. W. O'Loughlin, S. J. Pollock, T. H. Thatcher, S. E. Feldon and R. P. Phipps, Thy1 (CD90) controls adipogenesis by regulating activity of the Src family kinase, Fyn, *FASEB J.*, 2015, **29**, 920–931, DOI: **10.1096/fj.14-257121**.

71 D. A. Moraes, T. T. Sibov, L. F. Pavon, P. Q. Alvim, R. S. Bonadio, J. R. Da Silva, A. Pic-Taylor, O. A. Toledo, L. C. Marti, R. B. Azevedo and D. M. Oliveira, A reduction in CD90 (THY-1) expression results in increased differentiation of mesenchymal stromal cells, *Stem Cell Res. Ther.*, 2016, **7**, 97, DOI: **10.1186/s13287-016-0359-3**.

72 A. S. Zeiger, B. Hinton and K. J. Van Vliet, Why the dish makes a difference: Quantitative comparison of polystyrene culture surfaces, *Acta Biomater.*, 2013, **9**, 7354–7361, DOI: **10.1016/j.actbio.2013.02.035**.

73 R. J. McMurray, N. Gadegaard, P. M. Tsimbouri, K. V. Burgess, L. E. McNamara, R. Tare, K. Murawski, E. Kingham, R. O. C. Oreffo and M. J. Dalby, Nanoscale surfaces for the long-term maintenance of mesenchymal stem cell phenotype and multipotency, *Nat. Mater.*, 2011, **10**, 637–644, DOI: **10.1038/nmat3058**.

